Glycation of soy proteins leads to a range of fractions with various supramolecular assemblies and surface activities

Jilu Feng [a,b], Claire C. Berton-Carabin [b,c], Burçe Ataç Mogol [a], Karin Schroën [c], Vincenzo Fogliano [a,*]

[a] Food Quality and Design Group, Wageningen University and Research, Bornse Weilanden 9, Wageningen 6708 WG, the Netherlands
[b] INRAE, UR BIA, F-44316 Nantes, France
[c] Food Process and Engineering Group, Wageningen University and Research, Bornse Weilanden 9, Wageningen 6708 WG, the Netherlands

ABSTRACT

Dry and subsequent wet heating were used to glycate soy proteins with dextran or glucose, followed by fractionation based on size and solubility. Dry heating led to protein glycation (formation of furosine, Nε-(carboxymethyl)-ʟ-lysine, Nε-(carboxyethyl)-ʟ-lysine, and protein-bound carbonyls) and aggregation (increased particle size); while subsequent wet heating induced partial unfolding and de-aggregation. The measurable free amino group content of soy proteins changed from 0.77 to 0.14, then to 0.62 mmol/g upon dry and subsequent wet heating; this non-monotonic evolution is probably due to protein structural changes, and shows that this content should be interpreted with caution as a glycation marker. After both heating steps, the smaller-sized water-soluble fractions showed higher surface activity than the larger insoluble ones, and dextran conjugates exhibited a higher surface activity than their glucose counterparts. We thereby achieved a comprehensive understanding of the properties of various fractions in plant protein fractions, which is essential when targeting applications.

1. Introduction

The Maillard reaction (MR), also known as non-enzymatic browning, is a set of spontaneous and natural chemical reactions between the reducing groups of carbohydrates and the ε-amino groups of amino acids, peptides or proteins (Hodge, 1953). There is extensive evidence that Maillard conjugation (glycated proteins) can improve protein functionality, such as emulsifying, foaming, and gelling properties (Corzo-martínez, Carrera, Moreno, Rodríguez, & Villamiel, 2012; Spotti et al., 2019). Moreover, amphiphilic glycated proteins are able to form submicron particles via self-assembly upon heat treatment above the denaturation temperature of proteins (Feng et al., 2015; Li, Yu, Yao, & Jiang, 2008; Meng, Kang, Wang, Zhao, & Lu, 2018). Such Maillard conjugation-based submicron particles have been used as Pickering stabilizers or delivery vehicles to encapsulate and control release bioactive compounds (Fan, Yi, Zhang, & Yokoyama, 2018; Hernández, Santos, de Oliveira, Teófilo, & de Soares, 2020; Jin et al., 2016; Lin et al., 2019).

Most of the research on Maillard conjugation has been done on animal-derived proteins (e.g., whey protein isolate, β-lactoglobulin, bovine serum albumin, and egg white protein), focusing primarily on characterizing the improved protein functionality (Akhtar & Ding, 2017; Zhang et al., 2019a). Plant proteins are promising alternatives to animal proteins, due to the current trend in using more sustainable food ingredients. Yet, compared to animal proteins, the use of plant-based proteins for Maillard conjugation has been much less considered, and limited mainly to soy proteins, pea proteins and wheat proteins (Akhtar & Ding, 2017; Diftis & Kiosseoglou, 2006; Zha, Yang, Rao, & Chen, 2019). Among these, soy protein isolate (SPI) is the most widely used plant protein source owing to its good functional properties such as microencapsulation, emulsification, and gelation properties (Nesterenko, Alric, Silvestre, & Durrieu, 2013). It contains various proteins, with β-conglycinin and glycinin being the predominant ones. β-Conglycinin is a glycoprotein that consists of three subunits α, α' and β, which are randomly linked by non-covalent interactions (Thanh & Shibasaki, 1978). Glycinin is a hexamer, in which acidic and basic subunits are interconnected by a disulphide bond (Shewry, 1995).

Considering the compositional heterogeneity of SPI, as well as the complexity of the MR during which many molecular and supramolecular structure changes may occur, a vast number of components and products

are expected to be formed upon glycation. In most studies, proteins are incubated with carbohydrates and the whole reaction mixture is used without any post-reaction purification or fractionation. Some studies did use only the soluble fraction to prepare emulsions, to avoid the clogging of homogenization devices, taking into account the actual concentration after discarding the insoluble compounds (Wefers, Bindereif, Karbstein, & Van Der Schaaf, 2018; Weng et al., 2016). Yet, the insoluble fraction could be interesting for so-called Pickering emulsions or foams, for which insoluble colloidal particles are needed (Berton-Carabin & Schroën, 2015).

On the other hand, many studies have been carried out with limited chemical characterization and control of the extent of the MR and of the molecules and supramolecular structures (protein aggregates) formed. Some studies applied gel electrophoresis to confirm the conjugation between proteins and carbohydrates, although non-quantitatively (Lesmes & McClements, 2012; Xu, Wang, Jiang, Yuan, & Gao, 2012; Yadav, Parris, Johnston, Onwulata, & Hicks, 2010). A few authors attempted to limit the reaction to the initial stages: they estimated the degree of glycation quantifying free amino groups by the o-phthalaldehyde (OPA) or 2,4,6-trinitrobenzenesulfonic acid (TNBS) assays (Akhtar & Ding, 2017). Unfortunately, the free amino groups may be hindered as a result of protein aggregation, and thus prevented from reacting with the involved reagents, leading to an overestimation of the degree of glycation. Therefore, a direct measure of specific Maillard reaction products (MRPs) is mandatory to assess the extent of protein glycation.

The objectives of this study were to characterise the chemical and structural features of various Maillard reaction fractions (e.g., water-soluble vs insoluble, and differently glycated) and ultimately to propose optimal utilization of each fraction to minimise losses of precious materials. To achieve this aim in this paper, we first applied dry heating to induce Maillard conjugation between SPI and glucose or dextran (a large glucose-based polysaccharide), used in different ratios. The reaction products were separated by either centrifugation or filtration, and a second wet heat treatment was applied, as it was previously shown to alter the structural properties of the products formed in the first heating step, and thereby allow the formation of submicron particles (Feng et al., 2015; Li et al., 2008; Meng et al., 2018). A range of Maillard reaction markers was used to characterise the extent of the reaction (including free amino group, furosine, Nε-(carboxymethyl)-ʟ-lysine, Nε-(carboxyethyl)-ʟ-lysine, and protein-bound carbonyl contents) in all fractions. Surface hydrophobicity and tryptophan fluorescence were used to elucidate conformational changes, and interfacial tension between vegetable oil and water was assessed to prospective functionality in terms of stabilisation of multiphase food systems.

2. Materials and methods

2.1. Materials

Soy protein isolate (SPI, 79.14 ± 0.66% N; SUPRO® 500E) was obtained from Solae (St Louis, MO, USA). Protein concentration was determined by bicinchoninic acid (BCA) assay (Thermo Scientific, Pierce BCA Protein Assay Kit) or nitrogen determination by the Dumas method (Interscience Flash EA 1112 series, Thermo Scientific, Breda, The Netherlands). Refined rapeseed oil was purchased from a local supermarket (Wageningen, the Netherlands) and stripped with alumina powder (Alumina N, Super I, EcoChrome™, MP Biomedicals, France) to remove impurities and tocopherols (Berton, Genot, & Ropers, 2011). For sodium dodecyl sulphate-gel electrophoresis (SDS-PAGE), Mini-PROTEAN gels (12% TGX™ Gel, 10 well, 30 μL/well), precision plus protein™ standards (dual colour), Laemmli sample buffer, Tris/Glycine/SDS buffer, and Bio-safe™ Coomassie G-250 stain were supplied by Bio-Rad (Richmond, CA, USA). D-(+)-Glucose, dextran (average molecular weight 70 kDa), potassium bromide, β-mercaptoethanol, o-phtaldialdehyde, sodium tetraborate decahydrate, sodium dodecyl

sulphate (SDS), DL-dithiothreitol (DTT), ammonium formate, 2,4-dinitrophenylhydrazine (DNPH), guanidine hydrochloride, trichloroacetic acid (TCA), and 8-anilino-1-naphthalenesulfonic acid ammonium salt (ANSA) were purchased from Sigma-Aldrich (St. Louis, MO, USA), all at least of analytical grade. Analytical standard l-serine (99%) was supplied by Alfa Aesar (Wardhill, MA, USA), Nε-(2-furoylmethyl)-ʟ-lysine (furosine), Nε-(carboxymethyl)-ʟ-lysine (CML), Nε-(carboxyethyl)-ʟ-lysine (CEL), Nε-(2-furoyl)-methyl-l-[4,4,5,5-[$^{2}H_4$]lysine HCl salt (d$_4$-furosine), Nε-(carboxy[$^{2}H_2$]methyl)-ʟ-lysine (d$_2$-CML) were obtained from Polypeptide Group (Strasbourg, France), and Nε-(carboxy[$^{2}H_4$]ethyl)-ʟ-lysine (d$_4$-CEL) was purchased from Toronto Research Chemicals Inc. (Ontario, Canada). Hydrochloric acid (37%), ethanol (95%), ethyl acetate (99%), acetonitrile, and formic acid (98–100%) were from Merck Millipore (Merck, Germany). All solutions and dispersions were made using ultrapure water prepared with a Millipore Milli-Q water purification system (Millipore Corporation, Billerica, Massachusetts, US).

2.2. Preparation of glycated soy protein isolate

SPI and carbohydrate (glucose or dextran) powder mixtures with a weight ratio of 10:1, 2:1, or 1:1 were dispersed in water and lyophilized, after which the samples were milled with a Fritsch ball mill (Fritsch, Oberstein, Germany). The powder was subsequently incubated at 60 °C for 1 day at a relative humidity of 79% in a desiccator containing a saturated potassium bromide solution for protein glycation to take place, and next stored at −20 °C. Besides, the same procedure was used to make dry heated SPI that served as a control sample.

2.3. Fractionation of glycated soy protein isolate

A scheme of the samples prepared for the study is provided in Fig. 1. The glycated SPI samples or dry heated SPI samples were dispersed in water at 5 g/L, and gently stirred at 4 °C overnight to ensure full hydration. These dispersions were fractionated by centrifugation (10,000×g at 4 °C for 15 min; Sorvall Lynx 4000 Centrifuge, Thermo Scientific, Agawam, MA, USA) or filtration (Amicon stirred cell, Millipore Co., MA, USA, with Sterlitech polyethersulfone membranes, pore size 0.03 μm). The pellet and retentate were re-dispersed in a volume of water equivalent to the supernatant and filtrate, respectively. The pellet, supernatant, and retentate dispersions were heated in a water bath at 95 °C for 50 min to obtain the corresponding heated samples.

2.4. SDS-PAGE

A Mini-PROTEAN[e] Tetra system (Bio-Rad, Richmond, CA, USA) was used for SDS-PAGE analysis. First, samples (2 mg/mL protein content measured by BCA assay) were diluted 1:1 with Laemmli sample buffer containing 5% (v/v) β-mercaptoethanol and heated at 95 °C for 5 min on an Eppendorf ThermoMixer® C heating block (Eppendorf, Hamburg, Germany). Next, protein standard (10 μL) and sample solutions (20 μL) were loaded in separate wells in Mini-PROTEAN gels. The samples were separated at a constant voltage of 200 V at room temperature for approximately 30 min, after which the gels were stained with Coomassie G-250 for 1 h, and de-stained with water for 12 h. The gels were scanned using a GS-900™ Calibrated densitometer (Bio-rad, USA) and analysed with Image Lab 5.2.1 software (Bio-Rad, USA).

2.5. OPA assay

The free amino group content was estimated using the OPA assay as described by Nielsen, Petersen, and Dambmann (2001) with some modification. Briefly, 200 μL sample (solution or suspension) were added to 1.5 mL of freshly prepared OPA reagent (containing 38.1 g/L sodium tetraborate decahydrate, 0.8 g/L OPA, 1 g/L sodium dodecyl sulfate, and 0.88 g/L DL-dithiothreitol), and mixed on a digital vortex
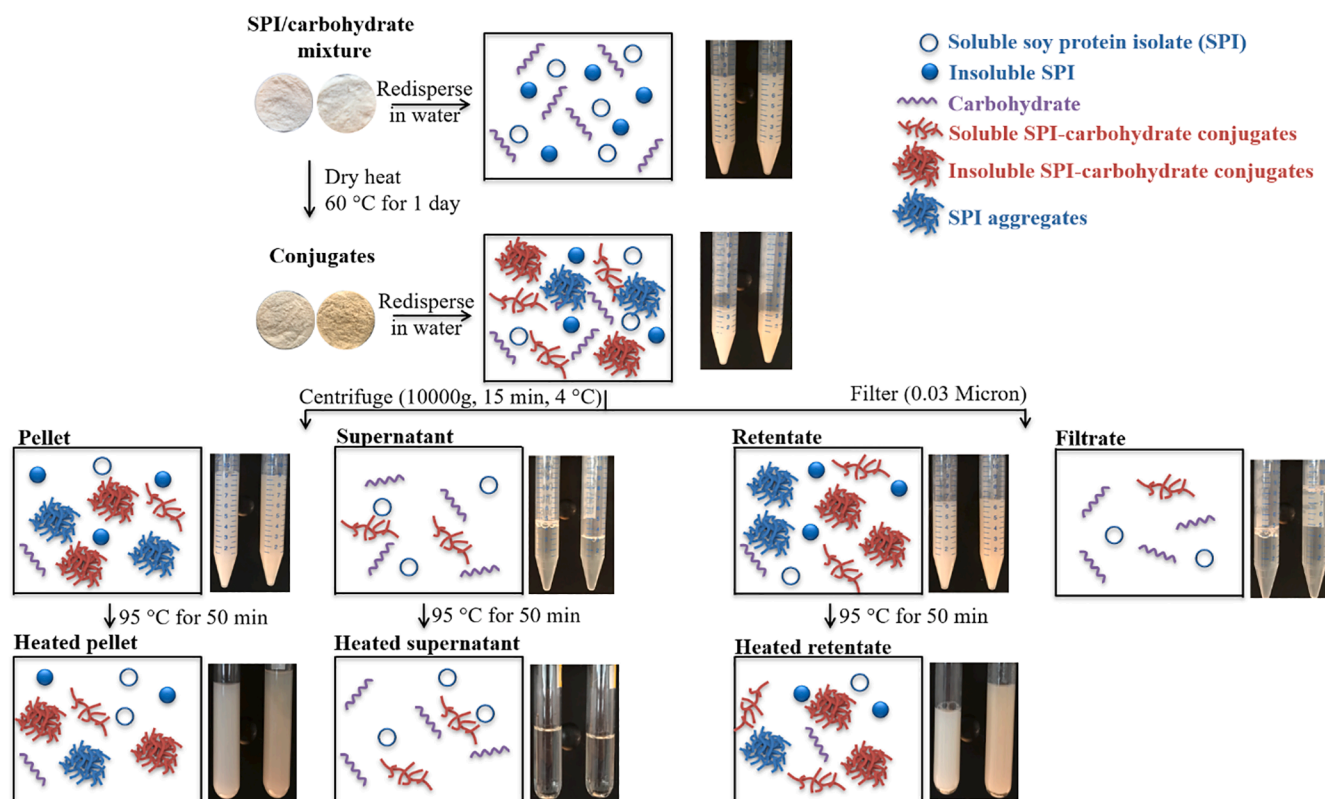
Fig. 1. Scheme of preparation of the different fractions. Photographs: Visual observations of SPI-dextran (left) and SPI-glucose (right) fractions.

mixer at 2500 rpm for 5 s. The mixture was incubated at room temperature for exactly 3 min, and the absorbance was measured at 340 nm using spectrophotometer DR3900 (Hach Lange, Germany). Calibration curves using L-serine as standard were used to determine the free amino group content expressed as millimole free amino groups per gram of protein (mmol/g protein). The protein concentration was determined with the BCA assay.

2.6. Analysis of Maillard reaction markers by LC-MS/MS

Analysis of furosine, CML, and CEL content was conducted on an Ultimate 3000 high-pressure liquid chromatograph (HPLC) (Thermo Scientific, USA) coupled to a Thermo Finnigan TSQ Quantum triple quadrupole mass spectrometer (San Jose, CA, USA) using the method of Troise, Fiore, Wiltafsky, and Fogliano (2015), with modifications. One millilitre of sample solution was mixed with 4 mL of 7.5 M hydrochloric acid (HCl) in a 10 mL heating tube and incubated at 110 °C for 20 h. To prevent oxidation, the heating tubes were saturated with nitrogen and sealed before incubation. Following incubation, the hydrolysates were filtered using syringe filters (PTFE, 0.22 Millipore, Billerica, MA, USA), after which filtrate aliquots (500 µL) were dried under nitrogen. The dried samples were reconstituted in 500 µL water. For SPI and SPI-dextran samples, 100 µL of the reconstituted sample was mixed with 90 µL of acetonitrile spiked with 10 µL internal standard. For SPI-glucose samples, a 10 µL reconstituted sample was mixed with 180 µL 50% (v/v) acetonitrile spiked with 10 µL internal standard. The final concentrations of internal standards in all samples were 500 µg/L furosine, 500 µg/L d_2-CML, and 200 µg/L d_4-CEL. Five microliters of each sample were injected into the LC-MS/MS system.

HPLC separation was performed using a reversed-phase core shell column (Kinetex HILIC 2.6 µm, 100 × 2.1 mm, Phenomenex, Torrance, USA). The mobile phases were: A, aqueous 0.1% (v/v) formic acid; B, 0.1% (v/v) formic acid in acetonitrile; C, 50 mM ammonium formate. The linear gradient elution steps were as follows: 0–0.8 min, 80% B, 10%

C; 0.8–3.5 min, 80–40% B, 10% C; 3.5–6.5 min, 40%B, 10% C; 6.5–8 min, 40–80% B, 10% C; 8–10 min, 80% B, 10% C. The flow rate was set at 0.4 mL/min, and detection was achieved by positive electrospray ionization using selected reaction monitoring (SRM). The source parameters were: spray voltage 3.0 kV, vaporizer temperature 250 °C, capillary temperature 310 °C, collision pressure 0.2 Pa, and scan time 100 ms. Data were analysed with Thermo Xcalibur 4.0.27.19 (Thermo Scientific, USA). The recovery of analytes was determined by spiking the samples with a known amount of analytes (low, middle, and high concentrations, corresponding to 30, 300, and 1000 ppb, respectively). Recovery experiments were repeated six times, and the results were $88.0 \pm 7.4\%$, $91.2 \pm 7.0\%$, and $84.2 \pm 6.1\%$ for furosine, CML, and CEL, respectively. Quantification of furosine, CML and CEL was performed by linear regression of the analyte/internal standard peak area ratio against analyte concentration. Protein content of each sample was measured by the Dumas method, and the final results were expressed as mg/g protein. Limit of detection (LOD) and limit of quantification (LOQ) were calculated based on the slope (S) of calibration curve and the standard deviation (SD) of responses according to Eqs. (1) and (2):

$$LOD = \frac{3.3 \times SD}{S} \tag{1}$$

$$LOQ = \frac{10 \times SD}{S} \tag{2}$$

The LOD were 0.2, 0.3, and 0.8 µg/L for furosine, CML, and CEL, respectively. The LOQ were 0.6, 1, and 2 µg/L for furosine, CML, and CEL, respectively.

2.7. Colour measurement

The colour change of SPI powder upon glycation was measured using a ColorFlex spectrophotometer (Hunter Associates Laboratory, Inc., Reston, VA, USA). Colour values were expressed according to the CIE lab

ARTICLE IN PRESS

J. Feng et al.   Food Chemistry xxx (xxxx) xxx

model, in which L^* (lightness), a^* (+a^* = red and - a^* = green) and b^* (+b^* = yellow and - b^* = blue) were recorded. The colour difference (ΔE) and browning index (BI) were calculated with Eqs. (3) and (4), respectively (Consoli et al., 2018).

$$\Delta E = \sqrt{\left(L^* - L_0^*\right)^2 + \left(a^* - a_0^*\right)^2 + \left(b^* - b_0^*\right)^2} \qquad (3)$$

where L_0^*, a_0^*, and b_0^* are the values before heat treatment, and L^*, a^*, and b^* are the values after dry heat treatment.

$$BI = \frac{x - 0.31}{0.172} \times 100 \qquad (4)$$

For x obtained from Eq. (5):

$$x = \frac{(a^* + 1.75L^*)}{(5.645L^* + a^* - 3.012b^*)} \qquad (5)$$

2.8. Determination of protein-bound carbonyl content

Protein-bound carbonyl content was measured by derivatization with DNPH following the method described by Duque-Estrada, Kyriakopoulou, de Groot, van der Goot, and Berton-Carabin (2020), with slight modification. Briefly, 0.8 mL of sample was precipitated with 0.8 mL of cold 40% (w/v) TCA in 2 mL Eppendorf tubes. The samples were centrifuged at 15,000×g for 5 min, the supernatant discarded, and SDS (400 μL, 5% (w/v)) was added to the pellet. The sample was then heated at 100 °C for 10 min and ultrasonicated (Elmasonic P 60H, Elma, Germany) at 40 °C for 30 min. For each sample, three aliquots were treated with 0.8 mL DNPH (0.3% (w/v) in 3 M HCl), and three with 0.8 mL 3 M HCl (blank). After incubating in the dark at room temperature for 1 h (while vortexing at 2500 rpm for 5 s every 10 min), 400 μL of cold 40% (w/v) TCA was added, and the sample was centrifuged as before. The supernatant was removed, and the pellet was washed with 1 mL of ethanol–ethyl acetate (1:1, v:v) solvent, and centrifuged as earlier, which was repeated thrice. The resultant pellet was dissolved in 1.5 mL 6 M guanidine hydrochloride and incubated overnight at 37 °C. Next, the sample was centrifuged (15,000×g, 5 min), and supernatant absorbance was recorded at 370 nm (spectrophotometer DR3900, Hach Lange, Germany). The supernatant protein concentration was measured with the BCA assay, and the protein-bound carbonyl content (mmol/kg soluble protein) was calculated using Eq. (6):

$$Carbonyl\,content = \frac{Ab_{sample} - Ab_{blank}}{\varepsilon \times l \times protein\,concentration} \qquad (6)$$

where Ab_{sample} and Ab_{blank} were the absorbances of the sample and blank, respectively, ε is the molar extinction coefficient of carbonyls (22,000 M^{-1} cm^{-1}) and l is the cuvette optical path (1 cm).

2.9. Surface hydrophobicity

Surface hydrophobicity of proteins in solutions or dispersions was measured by using ANSA as a fluorescence probe (Haskard & Li-Chan, 1998). The sample was diluted to the desired total protein concentration (0.05–0.25 mg/mL, measured with the BCA assay) using 0.01 mol/L phosphate buffer at pH 7.0, after which 40 μL ANSA stock solution (8 × 10^{-3} mol/L in 0.01 mol/L pH 7.0 phosphate buffer) were added to 2 mL of this diluted sample in a quartz cuvette. The mixtures were stirred with a magnetic bar and stored in the dark for 3 min before measurement. Fluorescence intensity was recorded at 390 (excitation) and 470 nm (emission) using a Shimadzu RF-6000 fluorimeter (Shimadzu, Kyoto, Japan) with slit widths of 5 nm for both excitation and emission. The initial slope of the fluorescence intensity (after blank subtraction) versus protein concentration (mg/mL) was obtained by linear regression analysis and used as an index of surface hydrophobicity.

2.10. Intrinsic fluorescence measurements

The intrinsic fluorescence of each sample was determined using the same fluorimeter as in 2.9 and based on the method of Tao et al. (2018). The excitation wavelength was 285 nm, and the intrinsic spectra were recorded between 300 and 400 nm at 60 nm/min scanning speed using slit widths of 5 nm. Prior to analysis, the samples were diluted to a protein concentration of 1 g/L (measured with the BCA assay) with phosphate buffer (0.01 mol/L, pH 7.0).

2.11. Adsorption kinetics

The interfacial tension between stripped rapeseed oil and aqueous solutions (protein concentration 0.1 g/L, measured with the BCA assay) was measured with an automated drop volume tensiometer (Tracker™, Teclis-IT Concept, Longessaigne, France) by analysing the axial symmetric shape (Laplace profile) of a rising oil drop (40 mm^2) in the aqueous solution. Prior to each experiment, the surface tension between air and water was measured (~72 mN/m) to ensure that the syringe, needle, and cuvette were clean. All measurements were conducted for 2 h at 20 °C.

2.12. Particle size distribution (PSD)

The size distribution of insoluble fractions was measured by a laser diffraction particle size analyser (Mastersizer 3000, Malvern Instruments, Worcestershire, UK), by dispersing in water and stirring at 1400 rpm in a dispersion unit (Hydro SM). The refractive indices of protein and water were 1.45 and 1.33, respectively. The absorption index of protein was set to 0.001.

The size distribution of soluble fractions was estimated by dynamic light scattering using a Zetasizer Ultra (Malvern Instruments, Worcestershire, UK). The samples were properly diluted in water to avoid multiple scattering before placing them in a disposable cell (DTS 1080) for analysis. The refractive and absorption indices used for protein were 1.45 and 0.001, respectively.

2.13. Statistical analysis

All measurements were done at least in triplicate on samples prepared at least in duplicate in independent experiments. The data were expressed as mean values ± standard deviation. Data were subjected to one-way analysis of variance (ANOVA) using the software package IBM SPSS statistics 23.0.0.2 (SPSS Inc, Chicago, Illinois, USA). The Tukey HSD method was conducted post-hoc for mean comparisons, with $P < 0.05$ being considered as significant. The lowercase letters in all figures are for comparison of different fractions within one system. The bold italic uppercase letters are for comparison between SPI and SPI-dextran systems, within the same fraction. The normal uppercase letters are for comparison between SPI and SPI-glucose systems within the same fraction.

3. Results and discussion

3.1. Free amino group content and supramolecular assembly state

At the early stages of the Maillard reaction, ε-amino groups of proteins react with carbonyl groups of reducing sugars to form so-called Amadori compounds (Silván, van de Lagemaat, Olano, & del Castillo, 2006). In SPI-carbohydrate mixtures (Fig. 2 A–D & S2), the free amino group contents significantly decreased ($P < 0.05$) after dry heating. Moreover, for SPI-dextran conjugates (Fig. 2A, 2C & S2A), higher amounts of free amino groups were measured compared to SPI-glucose conjugates (Fig. 2B, 2D & S2B). The decrease in free amino group content is generally interpreted in literature as a marker for protein glycation (Akhtar & Ding, 2017). The higher free amino group content in SPI-
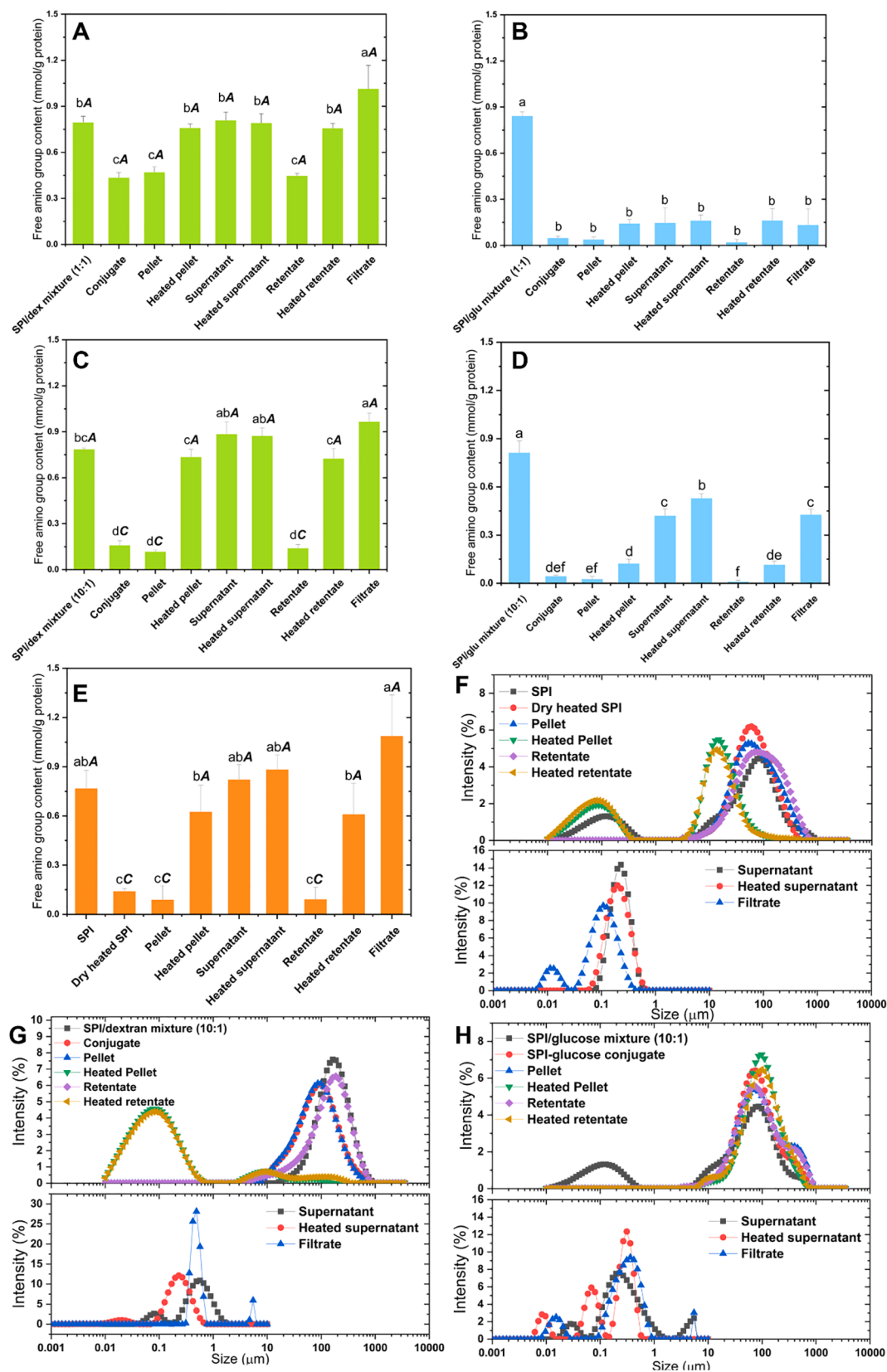
Fig. 2. (A-E) Free amino group content in different fractions of SPI-dextran (1:1) (A), SPI-glucose (1:1) (B), SPI-dextran (10:1) (C), SPI-glucose (10:1) (D), and SPI (E) systems, as measured by the OPA method. The lowercase letter is for comparison among different fractions in the same system. The uppercase letter is for comparison of SPI and dextran systems within the same fraction. Different letters indicate significant differences ($P < 0.05$). (F-H) Particle size distributions of different fractions of SPI (F), SPI-dextran (10:1) (G), and SPI-glucose (10:1) (H).

dextran than SPI-glucose conjugates could be explained by (i) at the same SPI-carbohydrate weight ratio, more glucose is present in the mixture than dextran due to its lower molecular weight, which ends up with more reducing end in the mixture, and thus glucose molecules are more likely to react with lysine residues of protein molecules; (ii) dextran is known to react slower than glucose, and (iii) long carbonic chain of dextran may limit protein glycation via steric hindrance (Wang & Ismail, 2012).

However, these results provide additional highlights: first, the second wet heating step applied to the insoluble fractions (i.e., pellet and retentate) increased the concentration of free amino groups (Fig. 2 & S2); and second, the apparent loss in free amino groups induced by dry heating is also observed in SPI where heated without carbohydrates (Fig. 2E). These results indicate that other mechanisms (apart from protein glycation) are responsible for the decrease in free amino groups detected by the OPA method. One possible explanation is the protein aggregation determined by thermal treatment as shown by the particle size of the SPI which dramatically increased upon heating (Fig. 2F). The aggregation determines the burying of amino groups inside the aggregates thus hindering access of the OPA reagent to free amino groups, as already reported for heated proteins (Mulcahy, Fargier-Lagrange, Mulvihill, & O'Mahony, 2017). This is also in line with the observation that the second wet heating increases the free amino group content. The heat treatment above the SPI denaturation temperature makes soy proteins unfold and de-aggregate, as is also clear from the decrease in particle size (Fig. 2F). Such a change in conformation and in supramolecular structure could help free amino groups becoming available again for the OPA reagent, which would thus counteract, at least in part, the effect observed during the first dry heating step.

Lower concentration of free amino groups per gram of protein was observed in all insoluble fractions (i.e., pellet and retentate) compared to soluble fractions (i.e., supernatant and filtrate) (Fig. 2). This is in line with the fact that the number of accessible free amino groups in aggregated protein clusters typical of the insoluble fractions would be lower than in the monomeric proteins present in the soluble fractions.

The outcomes of the OPA method are therefore indicative of a combined effect related not only to the degree of protein glycation, but also to the extent of protein aggregation a known, although too often underestimated, phenomenon, occurring during protein thermal treatment. To understand better the relationship between the extent of the MR and the functional properties of the glycated proteins it is thus important to measure other markers of the Maillard reaction, which is addressed in the next sections.

3.2. Quantification of MRPs as markers of the Maillard reaction

3.2.1. Furosine

Furosine [ε-N-(furoylmethyl)-l-lysine] is a specific marker for the early stages of the Maillard reaction, being representative of the concentration of the Amadori product glucosyl lysine (Erbersdobler & Somoza, 2007). As shown in Fig. 3, furosine was present (approximately 0.08 mg/g protein) in unheated SPI and unheated SPI/carbohydrate mixture, which is in agreement with Contreras-Calderón, Guerra-Hernández, and García-Villanova (2008), who reported similar values (0.06–0.33 mg/g of soy isolate). The presence of furosine in the starting samples is probably the result of thermal treatment applied during the production of SPI (Zhang et al., 2019b)

The concentration of furosine increased in all conjugates during the initial dry state heating (Fig. 3); the increase being considerably higher in glucose than in dextran conjugates (Fig. 3 A–D). As described earlier, glucose has more reducing ends than dextran and it is more reactive.

For glucose-based systems, no substantial differences in furosine content were found between the different SPI/glucose weight ratios tested (1:1, 2:1 and 10:1), whereas for dextran-based systems, the furosine content increased with decreasing the protein-to-dextran weight ratio (Figs. 3 & S3). The molecular weight of SPI is much

higher than that of glucose (ranging from around 200 000 to 600 000 g/mol for SPI, and 180.2 g/mol for glucose), and therefore the amount of glucose is already in excess and saturates the reactive sites of protein already at the lowest weight ratio of 10:1. This means that the protein concentration is the limiting factor for the formation of glucose-based Amadori compounds. Conversely, dextran (average molecular weight of 70,000 g/mol) has a molecular weight in the same range as that of SPI, leading to a higher concentration of Amadori compounds at higher dextran concentrations. In accordance with this, because of the large molecular weight and reactivity difference between both carbohydrates, the furosine content in the SPI conjugates was overall much lower with dextran than with glucose.

In glucose-based systems, the furosine content decreased after the second heat treatment (Figs. 3 & S3); this indicates that the related Amadori compounds degraded faster to intermediate and end products (Erbersdobler & Somoza, 2007), compared to dextran-based systems. This could be because the Amadori compound Nε-(1-Deoxy-D-fructos-1-yl)-L-lysine (fructosyl-lysine) evolves in intermediate and advanced MRPs, and the glucose present in the system does not have many other lysines to react with, thereby decreasing the overall furosine concentration. In addition, since glucose and dextran are hydrophilic and well soluble in aqueous media, the unreacted sugar molecules could be retained more in the soluble fractions, which could explain that the soluble fractions had a higher reactivity compared to insoluble fractions. It is clear that furosine is a sensitive marker for the early stages of the Maillard reaction, even when carbohydrates with low reducing activity such as dextran are used.

3.2.2. CML and CEL contents

The advanced stages of the Maillard reaction can be assessed through advanced glycation end products (AGEs), such as Nε-(carboxymethyl)-L-lysine (CML), and Nε-(carboxyethyl)-L-lysine (CEL). CML is formed mainly via two pathways: oxidation of fructosyl-lysine, and the direct reaction of glyoxal (GO) with lysine. CEL, a homolog of CML, is formed by the reaction of lysine with methylglyoxal (MGO). CEL and CML were present in the starting material (~0.09 and 0.08 mg/g protein, respectively) (Fig. S4), in line with the previously proposed effect due to a thermal treatment applied during the production of commercial SPI.

The concentrations of CML in SPI and SPI-dextran systems ranged from 7.00 to 40.4 mg/100 g of protein, while the values of CEL ranged from 4.80 to 25.0 mg/100 g of protein. CML and CEL contents in SPI-glucose systems were respectively ~ 10 and 5 times higher than in SPI-dextran systems, respectively. In the SPI-glucose system, CML and CEL contents could reach 396.3 and 138.6 mg/100 g of protein. To the best of our knowledge, there has not been other studies reporting CML and CEL contents in SPI-based systems. However, in powdered soybean-based feed products, CML and CEL contents were found to be 9.94 ± 0.74 and 0.98 ± 0.04 mg/100 g of protein, and increased to around 76 and 2.41 mg/100 g of protein, after being incubated at 110 °C for 60 and 45 min, respectively (Troise et al., 2015). This means that the concentrations of CML in SPI and SPI-dextran systems in our study was of the same order of magnitude as the ones reported by Troise and co-workers; while the CML and CEL contents in SPI-glucose systems were much higher than those reported by Troise et al. (2015). Glucose can directly oxidize to generate GO and MGO and further react with lysine to form CML and CEL, whereas dextran has first to be degraded into glucose units, then to be oxidized to induce GO and MGO (Fig. S4 A–F). In addition, dehydration from C3-C4 and C5-C6 of glucose molecules followed by retro-aldol cleavage can also generate GO (Yaylayan & Keyhani, 2000), which would also promote higher CML content in SPI-glucose systems than in SPI-dextran systems.

3.2.3. Colour

During the final stage of the Maillard reaction, melanoidins, i.e., brown nitrogenous polymers are formed, and hence the colour development is often used to get preliminary information on the extent of the
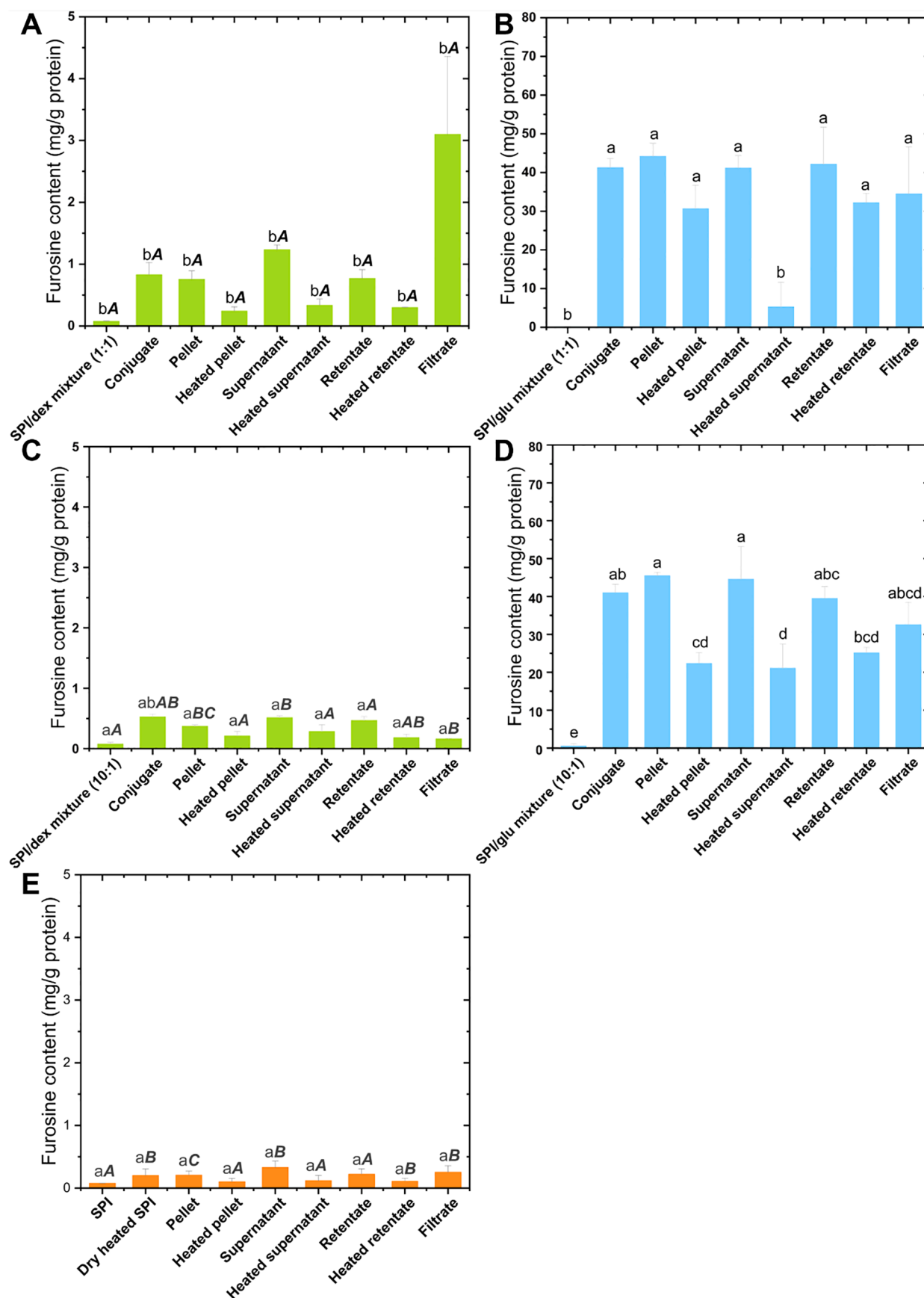
Fig. 3. Furosine content in different fractions of SPI-dextran (1:1) (A), SPI-glucose (1:1) (B), SPI-dextran (10:1) (C), SPI-glucose (10:1) (D), and SPI (E) systems. The lowercase letter is for comparison among the different fractions in the same system. The uppercase letter is for comparison of SPI and dextran systems within the same fraction. Different letters indicate significant differences ($P < 0.05$).

reaction in various samples. Colour formation is particularly relevant during the first heating step as shown in Table S1 for SPI and various mixtures with carbohydrates. Component b* that is indicative of yellowness increased in all samples upon heat treatment, though the increase in some dextran-based samples was not significant ($P > 0.05$). Especially in glucose-based systems, L* values (lightness) decreased and a* values (redness) increased, together with the results that higher colour difference and browning index were found in glucose-based systems than in dextran-based systems, indicating that the Maillard reaction proceeded further in the former ones, in line with the concentration of the various markers presented in Sections 3.2.1 and 3.2.2. These results corresponded with those reported previously where glycation of SPI with gum acacia or soy hull hemicelluloses resulted in an increase in a* and b* values and decrease in L* value, and these authors attributed the development of brown colour to the formation of brown polymers at the final stage of Maillard reaction (Li et al., 2015; Wang, Wu, & Liu, 2017).

3.2.4. Protein-bound carbonyl content

Maillard reaction generates α-dicarbonyl compounds that can also induce the deamination of amino acids, resulting in the oxidative damage of protein (Estévez, 2011). Protein-bound carbonyls are typically used as biomarkers of protein carbonylation.

The initial carbonyl content in SPI was relatively high, ~12 mmol/kg of protein before heat treatment (Fig. 4E). After the first heat treatment, the protein-bound carbonyl content of SPI-dextran systems was not significantly different ($P > 0.05$) from that of SPI (control), whereas SPI-glucose systems had 3–5 fold higher content than SPI (Figs 4 & S5). Liu, Xiong, and Butterfield (2000) reported a lower carbonyl level (6.4 mmol/kg of protein) for SPI, which is probably due to different processing methods used. In fact, they used freeze-dried SPI whereas the commercial SPI used in this study was prepared by spray drying; the latter being known to induce protein oxidation (Duque-Estrada et al., 2020). Carbonylation of proteins may occur via different pathways: first, oxidative deamination of amino acid side chains (e.g., lysine, arginine, threonine, and proline) via radical-mediation (Estévez, 2011). Second, α-dicarbonyl compounds formed by the Maillard reaction and/or sugar autoxidation may induce oxidative deamination (Akagawa, Sasaki, & Suyama, 2002). In the SPI-glucose systems, the MR was more intense, leading to more Amadori products and α-dicarbonyl compounds (Section 3.2), which eventually resulted in more severe protein oxidation.

Furthermore, we observed the simultaneous formation of CML, CEL, and protein-bound carbonyls (Table S2), which confirms that protein glycation and oxidation are intertwined. α-Aminoadipic semialdehydes (a typical protein oxidation product) can react with lysine residue through Schiff base formation or aldol condensation to form inter- and intra-molecular cross-links (Akagawa et al., 2002), indicating that protein oxidation is important in AGEs formation. Carbonylation of proteins is therefore only partially related to the MR development: therefore, in some food systems it is possible to find a correlation between the extent of protein carbonylation and the concentration of MRPs (like in this study) but in other systems for instance in fat-rich foods the two phenomena are rather separated.

3.3. Conformational changes

3.3.1. Surface hydrophobicity (H_0) analysis

Protein surface-exposed hydrophobicity is used to identify conformation changes, and is closely related to emulsifying and foaming properties of proteins. Upon dry heating at 60 °C, the surface hydrophobicity of SPI, SPI-dextran (10:1) and SPI-glucose (10:1) samples decreased by around 51%, 54%, and 67%, respectively (Fig. 5). The decrease in surface hydrophobicity could be due to the following reasons. (I) Covalent binding of the hydrophilic carbohydrates (i.e., dextran and glucose) to lysine residues via the Maillard reaction reduced the surface hydrophobicity of proteins; glucose being more potent than

dextran because SPI-glucose system contained more hydrophilic AGEs and melanoidins (Sections 3.2.2 and 3.2.3) (Chen, Chen, Wu, & Yu, 2016). (II) Glycation influences the isoelectric point of the protein, eliminating one positive charge on the free amino group, which reduces the repulsion among equally charged molecules (Davidov-Pardo, Joye, Espinal-Ruiz, & McClements, 2015). (III) Protein aggregation (see Section 3.1) that would reduce the exposure of hydrophobic sites on the protein surface.

In contrast with the first dry heating step, the second wet heating step has an opposite effect on surface hydrophobicity; a large increase in surface hydrophobicity was found for insoluble fractions of SPI and SPI-dextran systems (Fig. 5 A&B). This can be caused by (i) exposure of hydrophobic groups due to partial protein unfolding, and (ii) dissociation of SPI aggregates, therewith exposing hydrophobic groups that were previously hidden inside. These samples also showed relatively high free amino group content as discussed earlier (Section 3.1).

On the other hand, insoluble SPI-glucose systems did not show a change in surface hydrophobicity after the second heat treatment (Fig. 5C); most likely their high degree of glycation, and thus advanced, covalently modified reaction products, lead to a system with irreversibly formed protein aggregate (Section 3.2).

3.3.2. Intrinsic fluorescence analysis

To detect tertiary protein structure changes, the intrinsic fluorescence spectrum was determined. Depending on the microenvironment, the maximum emission (λ_m) can vary from 310 to 360 nm. When λ_m is lower than 330 nm, tryptophan (Trp) is considered to be in a nonpolar environment, while at $\lambda_m > 330$ nm, it is in a polar environment (Vivian & Callis, 2001). We found a λ_m of SPI of 333 nm (Fig. 5D), which is characteristic of a polar environment; similar results were reported by Shen and Tang (2012) who found 335.6 nm.

Upon the first dry heat treatment, the fluorescence intensity of SPI, SPI-dextran, and SPI-glucose conjugates decreased (Fig. 5 & Table S3). The second heat treatment at 95 °C resulted in a huge increase in fluorescence intensity of insoluble fractions (heated pellet and heated retentate) for SPI and SPI-dextran systems (Fig. 5 C&D), and in a small increase for SPI-glucose systems (Fig. 5E), which is in agreement with the surface hydrophobicity results. The decrease in intensity after the first heat treatment can be attributed to the aggregation of proteins, which shielded Trp residues in all samples. The shielding effect was more prominent in SPI-carbohydrate conjugates than dry heated SPI. It could be because the β-conglycinin and glycinin contain around 8 Trp residues located close to lysine residues (Keerati-u-rai, Miriani, Iametti, Bonomi, & Corredig, 2012), and carbohydrate molecules that react with those lysine residues via the Maillard reaction may block the fluorescent signal. No shift in λ_m was observed indicating that mild heat treatment (60 °C) did not greatly disrupt the protein structure. The second heat treatment may have caused unfolding of proteins and/or aggregate disassociation, thus exposing more hydrophobic groups leading to an increase in fluorescence intensity. Unfolding and dissociation of aggregates are less relevant for SPI-glucose systems, as argued in the previous section.

A slight blue shift of λ_m was observed for the insoluble fractions, indicating that the Trp residues were now present in a more nonpolar environment, for example within the hydrophobic core of aggregates. In the soluble fractions (supernatant, heated supernatant, and filtrate) there was a red shift of λ_m to 363–367 nm (Fig. 5 & Table S3) indicative of a more polar environment, although the overall effect was very low compared to that found for insoluble fractions.

3.4. Interfacial tension

Changes in the chemical and structural properties of proteins will affect their interfacial properties, herein assessed through interfacial tension measurements at the stripped rapeseed oil–water interface, and presented as semi-log plots (Fig. 6). Protein adsorption can be divided
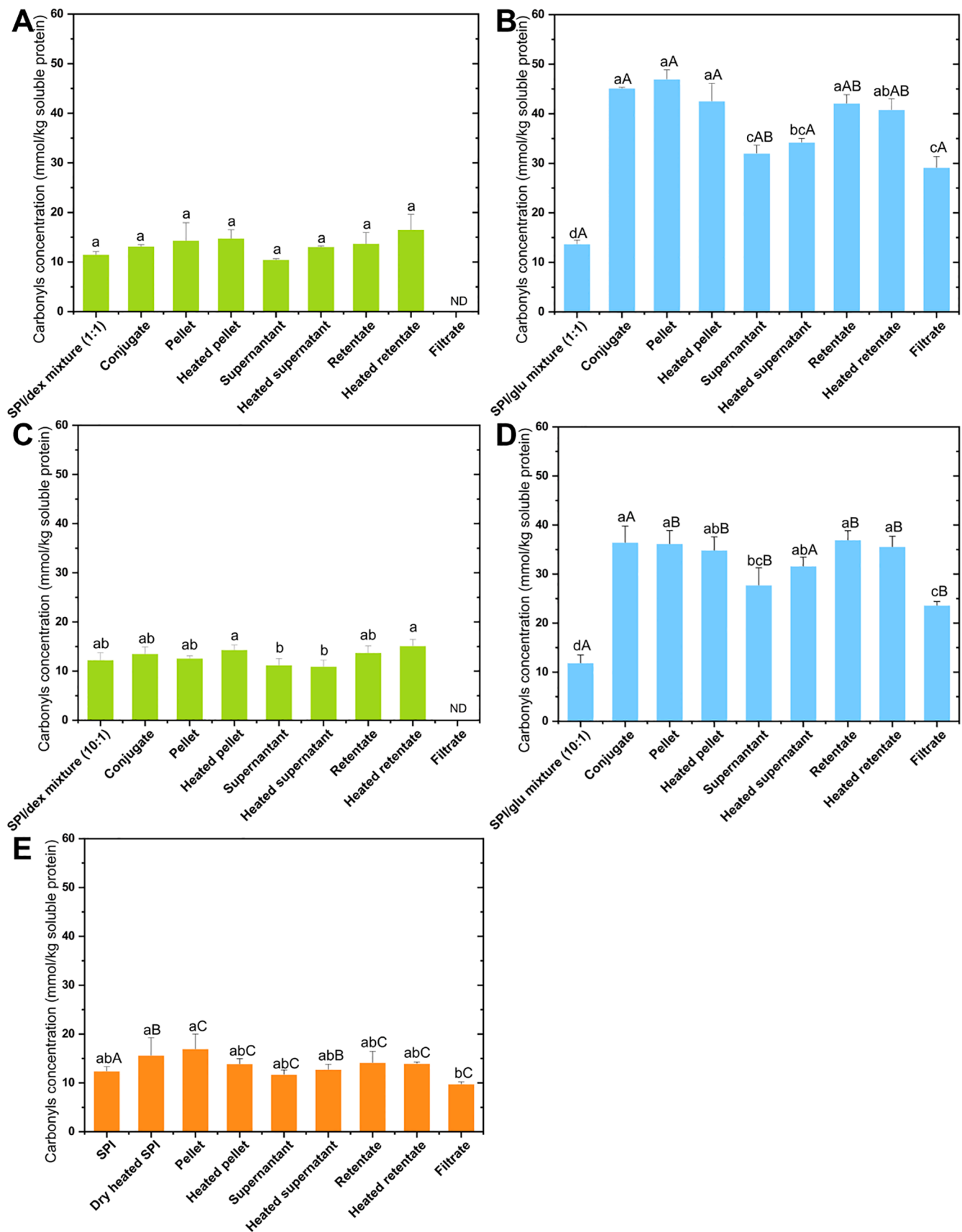
Fig. 4. Protein-bound carbonyl contents in different fractions of SPI-dextran (1:1) (A), SPI-glucose (1:1) (B), SPI-dextran (10:1) (C), SPI-glucose (10:1) (D), and SPI (E) systems. The lowercase letter is for comparison of different fractions in the same system. The uppercase letter is for comparison of SPI and SPI-glucose systems within the same fractions. Different letters indicate significant differences ($P < 0.05$).
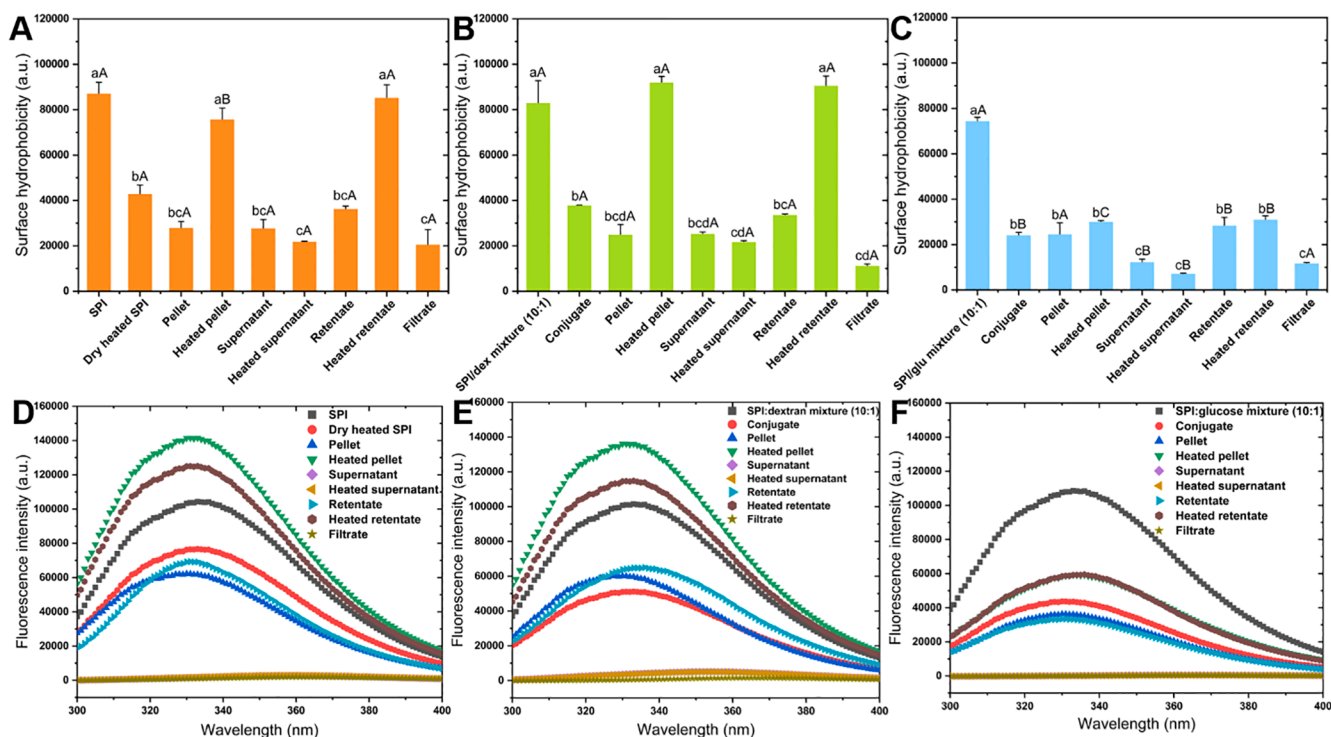
Fig. 5. (A-C) Protein surface-exposed hydrophobicity of SPI (A), SPI-dextran (10:1) (B), and SPI-glucose (10:1) (C) systems. The lowercase is for comparison among different fractions in the same system. The uppercase is for comparison among different systems with the same fraction. Different letters indicate significant differences ($P < 0.05$). (D-F) Emission fluorescence spectra (λ_{ex}: 285 nm) in aqueous dispersions for SPI (D), SPI-dextran (10:1) (E), and SPI-glucose (10:1) (F) systems.

into three stages (Beverung, Radke, & Blanch, 1999): (i) proteins diffuse from the bulk to the interface, and interfacial tension remains constant or decreases slightly during this so-called lag phase; (ii) as the interface gets covered with proteins, the interfacial tension decreases strongly while proteins may undergo conformational changes, rearrange and reorient; during stage (iii) protein molecules continue to change conformation and form a viscoelastic film, leading to a small decrease in interfacial tension.

The interfacial tension between stripped rapeseed oil and water was first confirmed to be stable at around 30 mN/m; no surface-active species were present (Fig. S6). In the presence of any of the samples (Fig. 6), interfacial tension progressively decreased, but no equilibrium was reached within 7200 s. The soluble fractions (i.e., supernatant, heated supernatant, and filtrate) had a shorter lag phase and decreased the interfacial tension faster than the insoluble fractions (e.g., pellet, retentate), indicating faster adsorption, which is logical given their smaller size (Fig. 1F-H), and expected ease of orientation at the interface. Conversely, insoluble fractions (pellet and retentate) had a larger particle size (Fig. 1F-H), and thus diffusion took more time. Furthermore, the insoluble fractions that were subjected to the second heat treatment (i.e., heated pellet and heated retentate) decreased interfacial tension slightly faster than the same samples without this treatment, which may be indicative of improved interfacial orientation due to higher exposed hydrophobicity (Section 3.3).

Protein glycation via the Maillard reaction was previously shown to improve the interfacial activity of soy β-conglycinin (Zhang, Wu, Yang, He, & Wang, 2012); however, in the present research, we only found small changes. Conjugation with dextran slightly increased the surface activity of SPI, but this was not the case with glucose (Fig. 6B&C). Since the extent of MR was high in the SPI-glucose system (Section 3.2), a large number of hydrophilic sugars were attached to the protein molecules, which decreased the surface hydrophobicity (Fig. 5C). For the dextran system, less glycation took place, and the molecule was more hydrophobic. This could explain the difference in surface behaviour.

However, also more protein aggregates appeared in the SPI-glucose systems than in the SPI-dextran systems (Section 3.1), which can also have reduced the observed surface activity. The surface activity can be changed using different fractions of glycated SPI results from different treatments (e.g., water-soluble and insoluble, dry and wet heating). This stresses the relevance of our research, and thus the importance of characterising components used for emulsion formulation, and that we found to hugely vary depending on the treatment that they received (even as a raw material).

4. Conclusions

The decrease in free amino groups upon protein glycation measured with OPA method was modulated by protein structural changes and should thus be interpreted with caution. Dry and subsequent wet heat treatment differently affect the protein products: dry heating of SPI and carbohydrate led to both protein glycation (as evidenced by the increase in furosine, CML, CEL, and protein-bound carbonyls) and protein aggregation (as evidenced by the decrease in free amino groups in SPI); while the subsequent wet heating above the denaturation temperature of SPI induced proteins to unfold and de-aggregate.

The surface activity of the fractions can be related to the surface hydrophobicity (fluorescence), with water-soluble fractions showing higher activity than insoluble fractions, as would be the case for dextran conjugates compared to their glucose counterparts. Heat treatment of the insoluble dextran fractions obtained after the Maillard reaction slightly improved surface hydrophobicity, and ability to lower surface tension due to unfolding and disaggregation most probably, but this was not the case for glucose conjugates that remained aggregated.

Therefore on one hand it is recommended to fractionate the complex reaction mixture for analysing it thoroughly using specific Maillard reaction markers, instead of the very general OPA method: on the other it is useful to link the chemical information to the functionality of different fractions. Based on this analysis, a comprehensive understanding of the
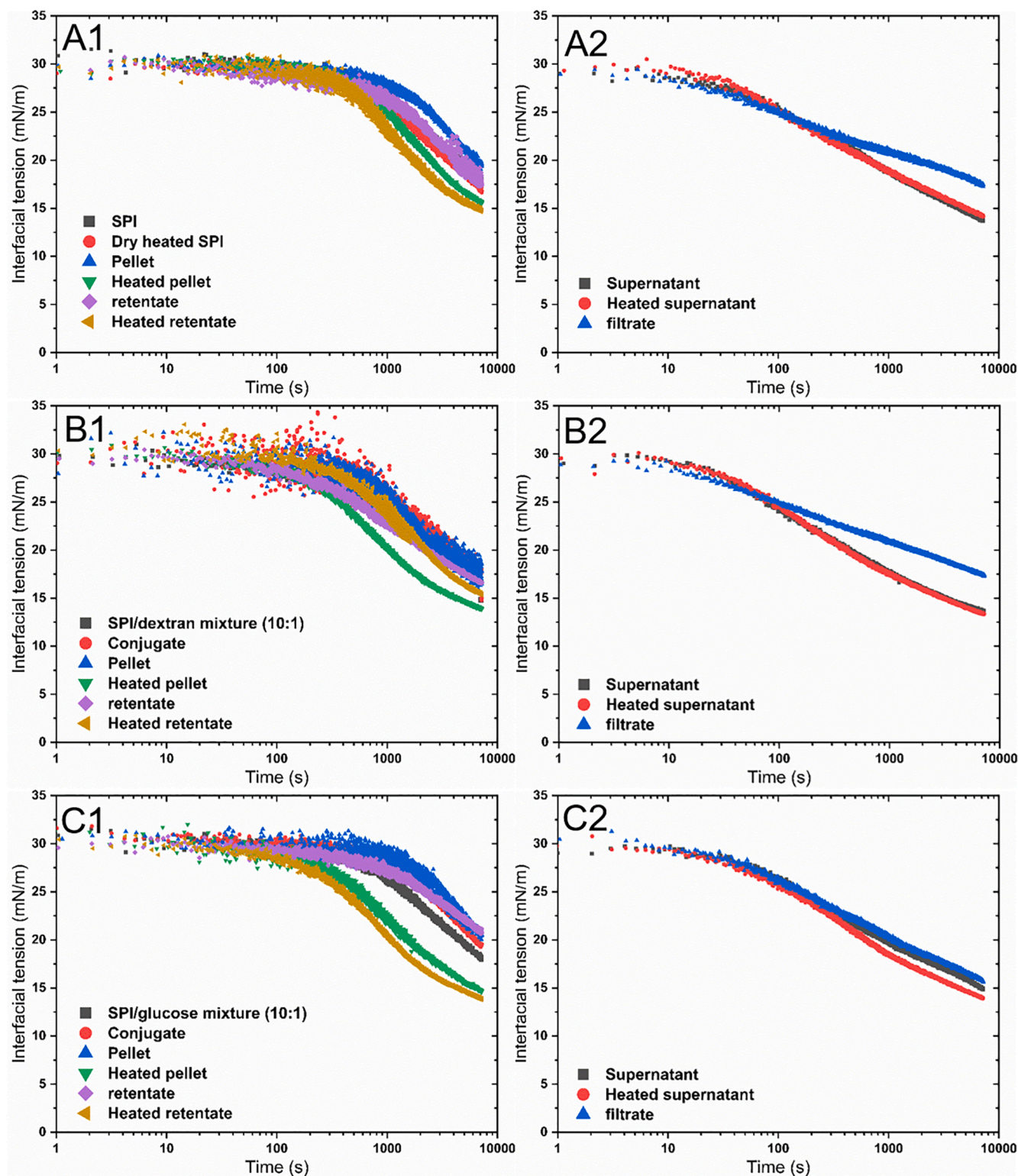
Fig. 6. Adsorption kinetics of the insoluble fractions (top) and soluble fractions (bottom) of SPI (A), SPI-dextran (10:1) (B), and SPI-glucose (10:1) (C) systems at the oil–water interface as a function of time (log scale). For clarity, only one representative curve is shown per sample, but similar results were obtained on multiple measurements using independent duplicates.

properties in each SPI fraction can be obtained, and a rational design of e.g., food emulsions and foams using different fractions of glycated plant proteins can be achieved. In this way, effective utilization of each fraction can be achieved to minimise losses of precious materials.

CRediT authorship contribution statement

Jilu Feng: Conceptualization, Methodology, Validation, Formal analysis, Investigation, Data curation, Writing - original draft, Visualization. **Claire C. Berton-Carabin:** Conceptualization, Methodology, Writing - review & editing, Visualization, Supervision. **Burçe Ataç**

ARTICLE IN PRESS

Mogol: Conceptualization, Methodology, Writing - review & editing, Visualization, Supervision. **Karin Schroën:** Conceptualization, Methodology, Writing - review - editing, Visualization, Supervision. **Vincenzo Fogliano:** Conceptualization, Writing - review & editing, Visualization, Supervision.

Declaration of Competing Interest

The authors declare that they have no known competing financial interests or personal relationships that could have appeared to influence the work reported in this paper.

Appendix A. Supplementary data

Supplementary data to this article can be found online at https://doi.org/10.1016/j.foodchem.2020.128556.

References

Akagawa, M., Sasaki, T., & Suyama, K. (2002). Oxidative deamination of lysine residue in plasma protein of diabetic rats: Novel mechanism via the Maillard reaction. *European Journal of Biochemistry, 269*(22), 5451–5458. https://doi.org/10.1046/j.1432-1033.2002.03243.x.

Akhtar, M., & Ding, R. (2017). Covalently cross-linked proteins & polysaccharides: Formation, characterisation and potential applications. *Current Opinion in Colloid & Interface Science, 28*, 31–36. https://doi.org/10.1016/j.cocis.2017.01.002.

Berton-Carabin, C. C., & Schroën, K. (2015). Pickering emulsions for food applications: Background, trends, and challenges. *Annual Review of Food Science and Technology, 6*(1), 263–297. https://doi.org/10.1146/annurev-food-081114-110822.

Berton, C., Genot, C., & Ropers, M. (2011). Quantification of unadsorbed protein and surfactant emulsifiers in oil-in-water emulsions. *Journal of Colloid and Interface Science, 354*(2), 739–748. https://doi.org/10.1016/j.jcis.2010.11.055.

Beverung, C. J., Radke, C. J., & Blanch, H. W. (1999). Protein adsorption at the oil/water interface: Characterization of adsorption kinetics by dynamic interfacial tension measurements. *Biophysical Chemistry, 81*(1), 59–80. https://doi.org/10.1016/S0301-4622(99)00082-4.

Chen, L., Chen, J., Wu, K., & Yu, L. (2016). Improved low pH emulsification properties of glycated peanut protein isolate by Ultrasound Maillard Reaction. *Journal of Agricultural and Food Chemistry, 64*(27), 5531–5538. https://doi.org/10.1021/acs.jafc.6b00989.

Consoli, L., Dias, R. A. O., Rabelo, R. S., Furtado, G. F., Sussulini, A., Cunha, R. L., & Dupas, M. (2018). Sodium caseinate-corn starch hydrolysates conjugates obtained through the Maillard reaction as stabilizing agents in resveratrol-loaded emulsions. *Food Hydrocolloids, 84*(June), 458–472. https://doi.org/10.1016/j.foodhyd.2018.06.017.

Contreras-Calderón, J., Guerra-Hernández, E., & García-Villanova, B. (2008). Indicators of non-enzymatic browning in the evaluation of heat damage of ingredient proteins used in manufactured infant formulas. *European Food Research and Technology, 227*(1), 117–124. https://doi.org/10.1007/s00217-007-0700-2.

Corzo-martínez, M., Carrera, C., Moreno, F. J., Rodríguez, J. M., & Villamiel, M. (2012). Interfacial and foaming properties of bovine b -lactoglobulin : Galactose Maillard conjugates. *Food Hydrocolloids, 27*(2), 438–447. https://doi.org/10.1016/j.foodhyd.2011.11.003.

Davidov-Pardo, G., Joye, I. J., Espinal-Ruiz, M., & McClements, D. J. (2015). Effect of Maillard conjugates on the physical stability of zein nanoparticles prepared by liquid antisolvent coprecipitation. *Journal of Agricultural and Food Chemistry, 63*(38), 8510–8518. https://doi.org/10.1021/acs.jafc.5b02699.

Diftis, N., & Kiosseoglou, V. (2006). Physicochemical properties of dry-heated soy protein isolate-dextran mixtures. *Food Chemistry, 96*(2), 228–233. https://doi.org/10.1016/j.foodchem.2005.02.036.

Duque-Estrada, P., Kyriakopoulou, K., de Groot, W., van der Goot, A. J., & Berton-Carabin, C. C. (2020). Oxidative stability of soy proteins: From ground soybeans to structured products. *Food Chemistry, 318*(February), Article 126499. https://doi.org/10.1016/j.foodchem.2020.126499.

Erbersdobler, H. F., & Somoza, V. (2007). Forty years of furosine - Forty years of using Maillard reaction products as indicators of the nutritional quality of foods. *Molecular Nutrition and Food Research, 51*(4), 423–430. https://doi.org/10.1002/mnfr.200600154.

Estévez, M. (2011). Protein carbonyls in meat systems: A review. *Meat Science, 89*(3), 259–279. https://doi.org/10.1016/j.meatsci.2011.04.025.

Fan, Y., Yi, J., Zhang, Y., & Yokoyama, W. (2018). Fabrication of curcumin-loaded bovine serum albumin (BSA)-dextran nanoparticles and the cellular antioxidant activity. *Food Chemistry, 239*, 1210–1218. https://doi.org/10.1016/j.foodchem.2017.07.075.

Feng, J.-L., Qi, J.-R., Yin, S.-W., Wang, J.-M., Guo, J., Weng, J.-Y., … Yang, X.-Q. (2015). Fabrication and characterization of stable soy β-conglycinin-dextran core-shell nanogels prepared via a self-assembly approach at the isoelectric point. *Journal of Agricultural and Food Chemistry, 63*(26). https://doi.org/10.1021/acs.jafc.5b01778.

Haskard, C. A., & Li-Chan, E. C. Y. (1998). Hydrophobicity of bovine serum albumin and ovalbumin determined using uncharged (PRODAN) and anionic (ANS-) fluorescent probes. *Journal of Agricultural and Food Chemistry, 46*(7), 2671–2677. https://doi.org/10.1021/jf970876y.

Hernández, H. L. H., Santos, I. J. B., Oliveira, E. B. de, Teófilo, R. F., Soares, N. de F. F., & Coimbra, J. S. dos R. (2020). Nanostructured conjugates from tara gum and α-lactalbumin. Part 1. Structural characterization. International Journal of Biological Macromolecules, 153, 995–1004. https://doi.org/10.1016/j.ijbiomac.2019.10.229.

Hodge, J. E. (1953). Dehydrated foods, chemistry of browning reactions in model systems. *Journal of Agricultural and Food Chemistry, 1*(15), 928–943. https://doi.org/10.1021/jf60015a004.

Jin, B., Zhou, X., Li, X., Lin, W., Chen, G., & Qiu, R. (2016). Self-assembled modified soy protein/dextran nanogel induced by ultrasonication as a delivery vehicle for riboflavin. *Molecules, 21*(3). https://doi.org/10.3390/molecules21030282.

Keerati-u-rai, M., Miriani, M., Iametti, S., Bonomi, F., & Corredig, M. (2012). Structural changes of soy proteins at the oil-water interface studied by fluorescence spectroscopy. *Colloids and Surfaces B: Biointerfaces, 93*, 41–48. https://doi.org/10.1016/j.colsurfb.2011.12.002.

Lesmes, U., & McClements, D. J. (2012). Controlling lipid digestibility: Response of lipid droplets coated by beta-lactoglobulin-dextran Maillard conjugates to simulated gastrointestinal conditions. *Food Hydrocolloids, 26*(1), 221–230. https://doi.org/10.1016/j.foodhyd.2011.05.011.

Li, C., Wang, J., Shi, J., Huang, X., Peng, Q., & Xueb, F. (2015). Encapsulation of tomato oleoresin using soy protein isolate-gum aracia conjugates as emulsifier and coating materials. *Food Hydrocolloids, 45*, 301–308. https://doi.org/10.1016/j.foodhyd.2014.11.022.

Li, J., Yu, S., Yao, P., & Jiang, M. (2008). Lysozyme−dextran core−shell nanogels prepared via a green process. *Langmuir, 24*(7), 3486–3492. https://doi.org/10.1021/la702785b.

Lin, Q., Li, M., Xiong, L., Qiu, L., Bian, X., Sun, C., & Sun, Q. (2019). Characterization and antioxidant activity of short linear glucan – lysine nanoparticles prepared by Maillard reaction. *Food Hydrocolloids, 92*(January), 86–93. https://doi.org/10.1016/j.foodhyd.2019.01.054.

Liu, G., Xiong, Y. L., & Butterfield, D. A. (2000). Properties of oxidized myofibrils and whey- and soy-protein isolates. *Journal of Food Science, 65*(5), 811–818.

Meng, J., Kang, T. T., Wang, H. F., Zhao, Bin, B., & Lu, R. R. (2018). Physicochemical properties of casein-dextran nanoparticles prepared by controlled dry and wet heating. *International Journal of Biological Macromolecules, 107*, 2604–2610. https://doi.org/10.1016/j.ijbiomac.2017.10.140.

Mulcahy, E. M., Fargier-Lagrange, M., Mulvihill, D. M., & O'Mahony, J. A. (2017). Characterisation of heat-induced protein aggregation in whey protein isolate and the influence of aggregation on the availability of amino groups as measured by the ortho-phthaldialdehyde (OPA) and trinitrobenzenesulfonic acid (TNBS) methods. *Food Chemistry, 229*, 66–74. https://doi.org/10.1016/j.foodchem.2017.01.155.

Nesterenko, A., Alric, I., Silvestre, F., & Durrieu, V. (2013). Vegetable proteins in microencapsulation: A review of recent interventions and their effectiveness. *Industrial Crops and Products, 42*(1), 469–479. https://doi.org/10.1016/j.indcrop.2012.06.035.

Nielsen, P. M., Petersen, D., & Dambmann, C. (2001). Improved method for determining food protein degree of hydrolysis. *Journal of Food Science, 66*(5), 642–646. https://doi.org/10.1111/j.1365-2621.2001.tb04614.x.

Shen, L., & Tang, C. H. (2012). Microfluidization as a potential technique to modify surface properties of soy protein isolate. *Food Research International, 48*(1), 108–118. https://doi.org/10.1016/j.foodres.2012.03.006.

Shewry, P. R. (1995). Plant storage proteins. *Biological Reviews, 70*(3), 375–426. https://doi.org/10.1111/j.1469-185x.1995.tb01195.x.

Silván, J. M., van de Lagemaat, J., Olano, A., & del Castillo, M. D. (2006). Analysis and biological properties of amino acid derivates formed by Maillard reaction in foods. *Journal of Pharmaceutical and Biomedical Analysis, 41*(5), 1543–1551. https://doi.org/10.1016/j.jpba.2006.04.004.

Spotti, M. J., Loyeau, P. A., Marangón, A., Noir, H., Rubiolo, A. C., & Carrara, C. R. (2019). Influence of Maillard reaction extent on acid induced gels of whey proteins and dextrans. *Food Hydrocolloids, 91*, 224–231. https://doi.org/10.1016/j.foodhyd.2019.01.020.

Tao, F., Jiang, H., Chen, W., Zhang, Y., Pan, J., Jiang, J., & Jia, Z. (2018). Covalent modification of soy protein isolate by (−)-epigallocatechin-3-gallate: Effects on structural and emulsifying properties. *Journal of the Science of Food and Agriculture, 98*(15), 5683–5689. https://doi.org/10.1002/jsfa.9114.

Thanh, V. H., & Shibasaki, K. (1978). Major proteins of soybean seeds. reconstitution of β-conglycinin from its subunits. *Journal of Agricultural and Food Chemistry, 26*(3), 695–698. https://doi.org/10.1021/jf60217a027.

Troise, A. D., Fiore, A., Wiltafsky, M., & Fogliano, V. (2015). Quantification of Nε-(2-Furoylmethyl)-l-lysine (furosine), Nε-(Carboxymethyl)-l-lysine (CML), Nε-(Carboxyethyl)-l-lysine (CEL) and total lysine through stable isotope dilution assay and tandem mass spectrometry. *Food Chemistry, 188*, 357–364. https://doi.org/10.1016/j.foodchem.2015.04.137.

Vivian, J. T., & Callis, P. R. (2001). Mechanisms of tryptophan fluorescence shifts in proteins. *Biophysical Journal, 80*(5), 2093–2109. https://doi.org/10.1016/S0006-3495(01)76183-8.

Wang, L., Wu, M., & Liu, H. (2017). Emulsifying and physicochemical properties of soy hull hemicelluloses-soy protein isolate conjugates. *Carbohydrate Polymers, 163*, 181–190. https://doi.org/10.1016/j.carbpol.2017.01.069.

Wang, Q., & Ismail, B. (2012). Effect of Maillard-induced glycosylation on the nutritional quality, solubility, thermal stability and molecular configuration of whey proteinv. *International Dairy Journal, 25*(2), 112–122. https://doi.org/10.1016/j.idairyj.2012.02.009.

Wefers, D., Bindereif, B., Karbstein, H. P., & Van Der Schaaf, U. S. (2018). Whey protein-pectin conjugates: Linking the improved emulsifying properties to molecular and physico-chemical characteristics. *Food Hydrocolloids, 85*(March), 257–266. https://doi.org/10.1016/j.foodhyd.2018.06.030.

Weng, J., Qi, J., Yin, S., Wang, J., Guo, J., Feng, J., … Yang, X. (2016). Fractionation and characterization of soy β-conglycinin-dextran conjugates via macromolecular crowding environment and dry heating. *Food Chemistry, 196*. https://doi.org/10.1016/j.foodchem.2015.10.072.

Xu, D., Wang, X., Jiang, J., Yuan, F., & Gao, Y. (2012). Impact of whey protein – Beet pectin conjugation on the physicochemical stability of β-carotene emulsions. *Food Hydrocolloids, 28*(2), 258–266. https://doi.org/10.1016/j.foodhyd.2012.01.002.

Yadav, M. P., Parris, N., Johnston, D. B., Onwulata, C. I., & Hicks, K. B. (2010). Corn fiber gum and milk protein conjugates with improved emulsion stability. *Carbohydrate Polymers, 81*(2), 476–483. https://doi.org/10.1016/j.carbpol.2010.03.003.

Yaylayan, V. A., & Keyhani, A. (2000). Origin of carbohydrate degradation products in L-alanine/D- [13C]glucose model systems. *Journal of Agricultural and Food Chemistry, 48*(6), 2415–2419. https://doi.org/10.1021/jf000004n.

Zha, F., Yang, Z., Rao, J., & Chen, B. (2019). Gum arabic-mediated synthesis of glyco-pea protein hydrolysate via Maillard reaction improves solubility, flavor profile, and functionality of plant protein. *Journal of Agricultural and Food Chemistry, 67*(36), 10195–10206. https://doi.org/10.1021/acs.jafc.9b04099.

Zhang, J. B., Wu, N. N., Yang, X. Q., He, X. T., & Wang, L. J. (2012). Improvement of emulsifying properties of Maillard reaction products from β-conglycinin and dextran using controlled enzymatic hydrolysis. *Food Hydrocolloids*. https://doi.org/10.1016/j.foodhyd.2012.01.006.

Zhang, Q., Li, L., Lan, Q., Li, M., Wu, D., Chen, H., … Yang, W. (2019a). Protein glycosylation: A promising way to modify the functional properties and extend the application in food system. *Critical Reviews in Food Science and Nutrition, 59*(15), 2506–2533. https://doi.org/10.1080/10408398.2018.1507995.

Zhang, W., Ray, C., Poojary, M. M., Jansson, T., Olsen, K., & Lund, M. N. (2019b). Inhibition of Maillard reactions by replacing galactose with galacto-oligosaccharides in casein model systems. *Journal of Agricultural and Food Chemistry, 67*(3), 875–886. https://doi.org/10.1021/acs.jafc.8b05565.